

Mareike Schreiber
Gerhard Schembecker*

Development of an Automated Adsorbent Selection Strategy for Liquid–Phase Adsorption

A systematic and automatic approach for adsorbent selection for liquid–phase adsorption is proposed. Based on physical properties like polarity, pore size, and specific surface, a screening strategy is developed and automated on a robotic platform. Key performance indicators are applied ensuring economically based decisions. The approach developed is verified by adsorption of caffeine out of an aqueous solution with vanillin, uracil, and α -ionon as impurities. The adsorbent selection strategy leads to the polymeric adsorbent SP207 and a specific surface of $15 \text{ m}^2 \text{ mL}^{-1}$ ending in a separation cost indicator of $16 \text{ € g}_{\text{Caffeine}}^{-1}$. This work proposes an opportunity for accelerated process design strengthened by the usage of robotic devices.

 This is an open access article under the terms of the Creative Commons Attribution-NonCommercial License, which permits use, distribution and reproduction in any medium, provided the original work is properly cited and is not used for commercial purposes.

Keywords: Automatic adsorbent selection, Downstream process design, Liquid-phase adsorption, Robotic platform

Received: March 22, 2022; *accepted:* April 05, 2022

DOI: 10.1002/ceat.202200152



Supporting Information
available online

1 Introduction

Over the last decades, in the field of process design for biochemical products the interest in automation increased significantly [1]. Automation benefits from shortened process development times, limited need of manual intervention, and lower material consumption. During downstream processing, automation is currently utilized for high-throughput (HT) experiments [2, 3], liquid and solid dosing steps [4, 5] as well as for single unit operations [6, 7] and for established processes [8].

The focus is shifting towards intelligent robotic devices combining HT experimentation with data management and evaluation resulting in autonomous robots for designing new production processes [9–11]. The robots should design self-determined the experiments necessary for the purification task given. They should process the data obtained autonomously leading to decisions for operating conditions, solvents, adsorbents or unit operations. Therefore, single unit operations should be designed automatically on robotic platforms with the ability of an extension to entire production processes.

In this context, ad- and desorption steps and here especially experimental screening of, e.g., adsorbents and solvents promise to benefit from laboratory automation. In principle, a high number of repetitive steps like dosing, weighing, shaking, and phase separation are necessary leading to great potential for automation [7]. Moreover, systematic and autonomous strategies for adsorbent and solvent selection reduce time and effort resulting in simplified process design.

Up to now, robotic devices specifically designed for solid-phase extraction (SPE) screen adsorbents in syringe, well plate, and column scale [12–14]. The emphasis is on fast data genera-

tion and HT experimentation for, e.g., designing chromatography steps. Therefore, liquid handling platforms are connected with resin screening kits equipped with minicolumn arrays or plates prefilled with chromatography media [15]. Mostly, the selection of adsorbents for a specific purification task is based on experience [7]. Either for manual or automated experiments, for every purification task a new set of adsorbents is chosen covering a broad range of physical properties [16–18]. To address these challenges, adsorption selection diagrams were developed leading to specific adsorbents for various applications [19]. Such selection diagrams differentiate between gas and liquid adsorption. For both cases, a more detailed subdivision is made for either impurity removal or bulk separation. Nevertheless, if no or only limited information is available for the system given, an appropriate preselection of adsorbents seems to be impossible.

To overcome the broad screening of a high number of different adsorbents for every new process, a universal approach is necessary for adsorbent screening and selection. In this work, a basic set of adsorbents for liquid-phase adsorption is defined applicable to a wide range of purification tasks. Furthermore, a general test strategy is developed experimentally, verified, and afterwards automated on a robotic platform. To rank and eval-

Mareike Schreiber, Prof. Dr.-Ing. Gerhard Schembecker
gerhard.schembecker@tu-dortmund.de
TU Dortmund University, Department of Biochemical and Chemical Engineering, Laboratory of Plant and Process Design, Emil-Figge-Str. 70, 44227 Dortmund, Germany.

uate the results, key performance indicators (KPIs) are utilized ensuring economically motivated and generalized decisions.

2 Materials and Methods

2.1 Robotic Platform

The custom-built robotic platform Lipos GXXL from Zinsser Analytics (Frankfurt, Germany) controlled by Zinsser WinLissy software is utilized for automated adsorption. The layout and features of the platform have been presented in detail in related publications [6,7,20]. An earlier study of Schuldt and Schembecker [7] proves that the robotic device is capable of executing an automatic, batchwise adsorption in 8-mL vials. For this, two pipettes are utilized with differently sized disposable tips (0.2 and 100 μL) for powder dosing. The principle of powder dosing on the robotic platform mentioned was described in detail before as well [7]. Further modules necessary for adsorption are two liquid dosing pipettes, an analytical scale, a centrifuge and a tempered shaking plate.

2.2 Model System

To verify the methodology developed for adsorbent screening, an aqueous solution containing dissolved caffeine (99 %, Alfa Aesar) with 500 mg L^{-1} , vanillin (99 %, Alfa Aesar) with 250 mg L^{-1} , uracil (>99 %, CalBiochem) with 100 mg L^{-1} and α -ionon (>90 %, Sigma Aldrich) with 50 mg L^{-1} was utilized for experimental purposes. Here, caffeine was the target component. Demineralized water was prepared with a Milli Q-Synthesis using Millipak-Express filter 0.22 μm (Merck Millipore).

2.3 Analytics

The samples obtained were analyzed by two high-pressure liquid chromatography (HPLC) systems (Knauer and Agilent) each equipped with a diode array detector and an EC 125/3 Nucleosil 100-5 C18 column (Macherey-Nagel). The oven temperature was set to 40 $^{\circ}\text{C}$. Prior to analysis, each sample was filtered by a syringe top filter (0.2 μm). The injection volume was 20 μL and the volume flow rate was 1 mL min^{-1} . Caffeine was detected at a wavelength of 275 nm after 2 min. The gradient applied can be seen in the Supporting Information (SI).

2.4 Adsorbents

The adsorbents used are listed in Tab. 1. Each adsorbent was washed prior to adsorption. Herefore, 6 g adsorbent was mixed with 30 g water. The mixture was shaken for 15 min in an overhead shaker (PTR-60, Grant Bio) at 60 rpm. After 15 min centrifugation at 4500 rpm (5804 R, Eppendorf), water and adsorbent were separated. The procedure was repeated four times whereas during the third repetition ethanol was utilized instead of water. Afterwards, the adsorbents were dried in a drying oven at 50 $^{\circ}\text{C}$ over night.

After washing, the adsorbents were preconditioned for the experiments. That is necessary due to the low wettability of the adsorbents with water. Accordingly, first the adsorbents were dosed referring to the desired specific surface (1, 5, and 15 m^2mL^{-1}). Then, 2.5 mL methanol was added, mixed, and removed. Afterwards, 7 mL demineralized water was added and removed repeatedly. The procedure ends in a wetted adsorbent in around 0.5 mL water.

Table 1. Adsorbents for screening experiments.

Adsorbent	Matrix	Specific surface $A_{\text{spez.}}$ [m^2g^{-1}]	Mean pore size d_{pore} [\AA]	Manufacturer
XAD7	Methacrylic polymers	450	90	Dow / Rohm & Haas
XAD16	Styrene-divinylbenzene copolymers	900	100	Dow / Rohm & Haas
SP207	Styrene-divinylbenzene copolymers (Br)	650	105	Mitsubishi
PAD950	Methacrylic polymers	450	130	Purolite GmbH
DAX8	Methacrylic polymers	140	225	Sigma Aldrich
HP20SS	Styrene-divinylbenzene copolymers	500	260	Mitsubishi
PAD610	Polyacrylic polymers	490	290	Purolite GmbH
XAD1180	Styrene-divinylbenzene copolymers	600	300	Dow / Rohm & Haas
Activated carbon	Carbon	498 ^{a)}	Broad pore size distribution	Alfa Aesar
Silica gel	Silicon dioxide	550	60	Supelco

^{a)} BET surface measured via Gemini 2360 surface area analyzer

2.5 Key Performance Indicators

To ensure economic rating during early process design stages, Winkelkemper and Schembecker [21] derived a relation between purification performance, experimental yield, and specific costs for upstream and downstream. In this context, the purification performance index (PPI_i)¹⁾ was introduced to describe the purity performance of a process step or step combination (Eq. (1)). The PPI_i rates the purity from input x_{in} to output x_{out} in the boundaries of initial x_0 and target purity x_f [21].

$$PPI_i = \frac{\tanh^{-1}(2x_{out,i} - 1) - \tanh^{-1}(2x_{in,i} - 1)}{\tanh^{-1}(2x_f - 1) - \tanh^{-1}(2x_0 - 1)} \quad (1)$$

The process performance can be accessed without the need of an entire process concept by the separation cost indicator (SCI_i). Therefore, experimental yield Y , specific costs κ , and PPI_i are combined resulting in an indicator for the economic efficiency of the process (Eq. (2)) [21].

$$SCI_i = Y_i^{PPI_i} \left(\kappa_{conv.} + \kappa_{pur.,i} \frac{1 - Y_i^{PPI_i}}{1 - Y_i} \right) \quad (2)$$

The most efficient process steps and operating conditions are indicated by a low SCI_i . The SCI_i is applied to compare the performance of several adsorbents at varying specific surfaces. Further information concerning the assumptions and parameters for SCI_i calculation can be found in the SI.

3 Approach for Autonomous Adsorbent Selection

During the design of ad- and desorption steps, adsorbent selection influences greatly the efficiency of the entire process right from the start. If only limited information is available about the system to be purified, e.g., a complex fermentation broth with various impurities and a new target component, a specific and, at the same time, fast adsorbent selection is impossible. Up to now, adsorbents are chosen individually for different purification tasks leading to high experimental effort and material consumption. Furthermore, for prediction of multicomponent adsorption isotherms single component isotherms must be measured leading to a highly time-consuming method [22]. Thus, the focus of this work is on defining a representative set of adsorbents and developing a systematic screening strategy for various applications for liquid-phase adsorption. Additionally, criteria are defined to eliminate non-suitable adsorbents directly in the beginning. The number of experiments is minimized by obtaining the degree of information necessary for appropriate adsorbent selection. Overall, the methodology developed will be executed automatically on a robotic platform.

During biochemical process design, adsorption is mostly applied to recover target components from an aqueous supernatant [18, 23, 24]. Therefore, as much as possible target product should be separated from that solution leading to capture mode as preferred operating mode. Since fermentation broths, besides of water, contain several impurities like, e.g., salts, solubilizers or byproducts with similar properties as the product, it is advantageous to screen different adsorbent classes.

Technical adsorbents are classified into carbon-based, oxidic, and polymeric materials [25]. Based on a broad spectrum of chemical and physical properties, affinity and capacity for varying material systems differ for different adsorbents. In particular, a high degree of microporosity combined with high adsorption capacity are promising features of carbon-based adsorbents. Thus, they are suitable for, e.g., adsorption of organic molecules [16]. However, due to low abrasion resistance, low purity, high production and regeneration costs, other adsorbents are more likely to be used nowadays [16, 25].

Oxidic adsorbents provide low production costs, high stability in basic solutions, and fixed pore structures. They are applied almost exclusively in gas-phase adsorption processes [25]. The benefit of polymeric adsorbents lies in precise adjustment of physical properties due to their synthetic production. They have high adsorption capacities and are utilized during gas- and liquid-phase adsorptions. Nevertheless, due to their high production costs they are mostly applied for high-value products [25]. Overall, a representative set of adsorbents for various purification purposes should contain adsorbents of each category mentioned. Thereby, a broad range of physical properties will be covered ranging from oxidic resins and activated carbons to polymeric resins with different surface functionalization.

Yield and selectivity describe the performance of an adsorption step. The affinity of adsorbent and adsorbate to interact, the adsorption strength, is influenced by the polarity of both. Moreover, the surface area available for adsorption determines the yield. Selectivity is a result of differences in adsorption strength for the molecules involved. Kinetic and thermodynamic effects, like different diffusion rates, affect such adsorption strength. Based on different pore structures and pore sizes, steric effects might lead to different adsorption rates or even steric hindrance of molecules [25, 26].

Whereas on molecular level, such distinction between the different impact factors on the separation performance seems reasonable, on process level certain interactions must be considered. For example, selectivity depends on the surface area available, too. In capture mode, the more area is provided, the more the yield will improve. On the other side, the selectivity might go down as more impurities might be adsorbed. Such interactions make the design of an adsorption process highly complex and time-consuming. Since the effects mentioned are mutually dependent, the adsorption strength and efficiency can not be predicted straightforward. Numerous experiments are necessary to fully understand all these effects. Therefore, a fast, easy-to-automate design procedure for adsorption processes requires simplifications. Nevertheless, a promising screening procedure must consider thermodynamic and kinetic effects as well as available surface area simultaneously.

Taking into account the different adsorbent categories mentioned, a representative set of adsorbents is defined (see Tab. 1).

1) List of symbols at the end of the paper.

Based on the preliminary considerations, the polarity of an adsorbent is utilized as a measure for the different thermodynamic properties of adsorbents (e.g., binding energies). Differences in kinetic and steric properties are considered by taking into account differences in the pore size of adsorbents. This simplification allows classifying existing adsorbents into four groups: I) low polarity, large pores; II) high polarity, large pores; III) low polarity, small pores; IV) high polarity, small pores (see Fig. 1). The impact factor surface area is taken into account by changing the specific adsorption surface per volume of fluid during the experiments.

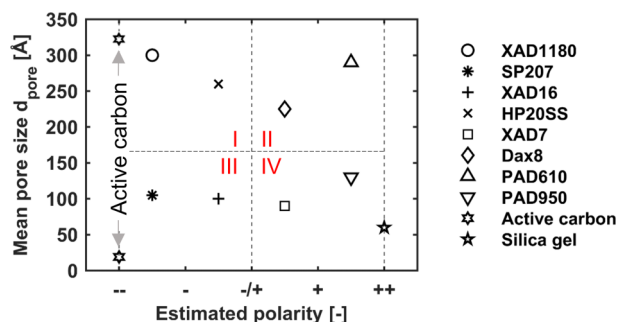


Figure 1. Basic set of adsorbents for systematic screening. Adsorbents are categorized into four groups I–IV according to their mean pore sizes (low around 100 Å, large around 250 Å) and estimated polarity (low-polar --/–, high-polar +/++) based on their surface functionalization and dipole moments.

Regarding the polarity, a little bit finer classification into low-polar (–/–) and high-polar (+/++) is introduced. This seems to be justifiable as the polarity of adsorbents is characterized by their surface functionalization and their dipole moments. The detailed grouping into (–↔–) / (–↔±) / (±↔+) / (+↔++) and thus the range of polarity considered is based on information from the suppliers' data sheets. For example, for the polymeric low-polar amberlite resin SP207 bromination leads to a lower polarity compared to XAD16. Inside the same polarity class (–↔–) / (–↔±) / (±↔+) / (+↔++), the adsorption performance will differ due to slight differences in dipole moment leading to different bonding capacities. However, for simplicity reasons, all adsorbents out of the representative set with similar polarities are arranged centrally in one sub-class only differing in their mean pore sizes. Therefore, each polarity class in Fig. 1 includes two representative adsorbents, one with a higher (around 250 Å) and one with a lower mean pore size (around 100 Å).

Extreme polarity properties (polarity classes -- and ++) are covered by active carbon and silica gel. Due to the broad pore size distribution of active carbon, it is arranged over the total range of mean pore sizes. In the following, each adsorbent is specified by a group I–IV and a polarity sub-class (–↔–) / (–↔±) / (±↔+) / (+↔++). Although the representative set of adsorbents selected is worth discussing, the set chosen offers a good starting point for process design, simplifying and accelerating adsorbent selection.

In order to determine reasonable values for the surface area offered for a dedicated adsorption, existing adsorption processes

were evaluated extracting the surface offered per volume of fluid [7, 18]. Combining the data with preliminary experiments results in three different sorbent-to-fluid ratios (1, 5, 15 m²mL⁻¹) screened equally for all adsorbents. Hereby, the trend and effect of increasing surface on yield is tracked sufficiently. Due to the broad range of 1–15 m²mL⁻¹, the effect of competing adsorption on yield and respectively selectivity of a multicomponent mixture is investigated as well. The maximum specific surface area of 15 m²mL⁻¹ was selected to avoid very high cost for adsorbent material. To be able to compare the performance of different adsorbents, the amount of fluid is fixed to 5 mL in each experiment. Then, the masses of the adsorbents are varied to reach the above-mentioned sorbent-to-fluid ratios. All experiments were performed at room temperature (20–25 °C) and lasted 120 min aiming at low operating costs and limited processing time.

The contribution focuses on separation of target molecules out of fermentation broths. Consequently, for all experiments, the target phase is the adsorbent and thus the adsorption is executed in capture mode. Therefore, the approach focuses primarily on high yield for the target component. However, in multicomponent mixtures, competing adsorption of target component and impurities cannot be neglected. By variation of mean pore sizes and surface area during the screening, investigations of steric hindrance and competing adsorption effects on selectivity and thus purity of the target component are implied. Additionally, the varying specific surfaces of the adsorbents from 140–900 m²g⁻¹ are leading to significant differences in masses dosed and variable costs (see Tab. 1, SI). Thus, the costs for the adsorbents used should be taking into account as well. The combination of all three factors is leading to the SCI_i (see Sect. 2.5). The SCI_i is highly sensitive to yield changes, especially in the range of 80–90 %. A purity increase and thus selective adsorption of the target component is indicated by a positive PPI_i . The specific costs for purchasing and recycling of the adsorbents are included, too. The SCI_i decreases for increasing yields and PPI_i .

Although possible when using an automated laboratory robot, screening the full set of representative adsorbents should be avoided to minimize time, effort, and material consumption. Therefore, a strategic approach is proposed as shown exemplarily in Fig. 2 focusing on a minimal SCI_i . During the screening, polarity, mean pore size and surface area are varied in order to identify the most economical combination meaning a minimal SCI_i . The screening order is adapted based on the SCI_i and is always redirected according to the values obtained. As soon as the SCI_i increases compared to the previous screening step, the search is terminated.

Exemplarily, one screening scenario is explained in detail in the following (see Fig. 2):

- 1) For each purification task, the screening starts with testing two medium polar adsorbents XAD16 (III, (–↔±)) and XAD7 (IV, (±↔+)). They are tested at varying specific surface areas (1, 5, and 15 m²mL⁻¹). The two are chosen for initial screening due to their comparatively low purchasing costs (€m⁻²) compared to the adsorbents in the same polarity classes with large pores (HP20SS and Dax8). Based on the lowest SCI_i , determined by the minimum of three different specific surface areas, one polarity side, either low-

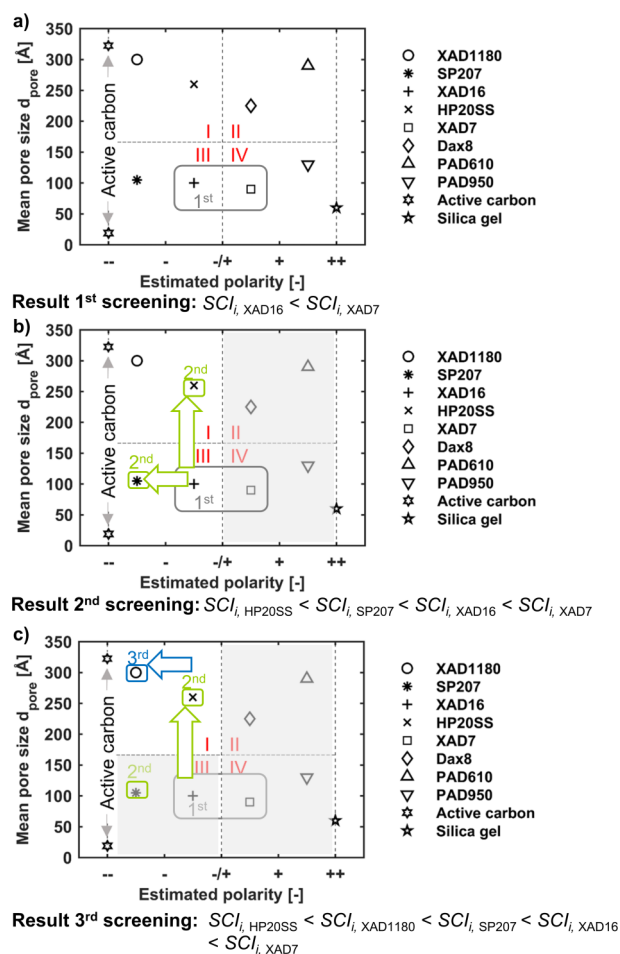


Figure 2. Stepwise adsorbent screening at varying specific surfaces of 1, 5, and 15 m²mL⁻¹ targeting at minimal SCI_i . (a) Starting point of the screening are XAD7 and XAD16. The search for the minimal SCI_i determines group I/III for further screening. (b) Stepwise screening of adsorbents with lower polarity or higher pore size. Fixing of mean pore size to large pores (I). Adjustment of search direction according to the minimal SCI_i . (c) Screening of adsorbent with same pore size but different polarity. Search terminates due to increasing SCI_i .

polar ($-\leftrightarrow\pm$) or high-polar ($\pm\leftrightarrow++$), is excluded entirely from further screening. In Fig. 2a, exemplarily the SCI_i for XAD16 (III, ($-\leftrightarrow\pm$)) is lower and thus the adsorption tends to be more economical with XAD16. Therefore, XAD7, PAD950, Dax8, PAD610, and silica gel are excluded.

- The second screening always focuses on fixing the mean pore size to reduce the number of varying impact factors. To investigate simultaneously the influence of polarity and mean pore size on adsorption performance, HP20SS (I, ($-\leftrightarrow\pm$)) and SP207 (III, ($-\leftrightarrow-$)) are tested in the next screening step (see Fig. 2b). In case of a steric effect, the yield should be higher for HP20SS (I, ($-\leftrightarrow\pm$)) compared to XAD16 (III, ($-\leftrightarrow\pm$)). Nevertheless, the higher pore size could also lead to a higher adsorption of impurities in case of a prior steric hindrance resulting in a decreased PPI_i . Additionally, the polarity is decreased by the usage of

SP207 (III, ($-\leftrightarrow-$)). To rate all effects mentioned at once, the SCI_i is applied. In the example given, the SCI_i of HP20SS (I, ($-\leftrightarrow\pm$)) is lower compared to all previous values. Thus, large pore sizes are advantageous indicating a steric hindrance during adsorption with small pore sized adsorbents and SP207 (I, ($-\leftrightarrow-$)) is excluded from further screening. Here, the search direction is adjusted depending on the SCI_i towards large mean pore sizes.

- At this stage, it may be that adsorbents with small pore sizes and low polarity just led to higher SCI_i because a steric effect inhibited adsorption of the target component. Since a possible steric effect is compensated by large pore sizes, the influence of polarity on adsorption strength is investigated further. If the minimum is not identified, XAD1180 (I, ($-\leftrightarrow-$)) will be screened and the SCI_i will be compared to the previous values (see Fig. 2c). In the example given, the SCI_i of XAD1180 is higher compared to HP20SS. Thus, the search terminates and HP20SS (I, ($-\leftrightarrow\pm$)) is chosen for an adsorption step with the surface resulting in the minimal SCI_i of the adsorbents tested.

The strategy would be exactly mirrored, referring to Fig. 2, if the SCI_i for XAD7 (IV, ($\pm\leftrightarrow+$)) was lower. In case of an insignificant difference between XAD16 (III, ($-\leftrightarrow\pm$)) and XAD7 (IV, ($\pm\leftrightarrow+$)) the same screening procedure is applied for both sides ($-\leftrightarrow\pm$) and ($\pm\leftrightarrow+$) (see SI). As soon as a significant difference between non-polar and polar adsorbents is identified, one polarity is excluded from further screening. Hereby, the number of experiments is reduced by obtaining a flexible screening procedure. The strategy adapts autonomously to a particular task ensuring cost-driven decisions. The methodology provides a reliable start for designing an adsorption-desorption process. The adsorbents selected cover a broad range of physical properties. Further adsorbents could be added to the set for already well-established adsorption processes.

4 Results and Discussion

The strategy developed is applied and verified by adsorption of caffeine out of an aqueous solution. All sorbents are washed and preconditioned according to Sect. 2.4. First, the experiments are performed manually (Sect. 4.1). Afterwards, the strategy is implemented in the workflow of the robotic platform for complete automation targeting at autonomous process design (Sect. 4.2). Values necessary for calculation of the SCI_i , like yield, purity, and PPI_i , are listed in Tab. 2 and in the SI.

4.1 Verification of Adsorbent Selection Strategy

According to the methodology developed in Sect. 3, XAD16 (III, ($-\leftrightarrow\pm$)) and XAD7 (IV, ($\pm\leftrightarrow+$)) are tested initially at 1, 5, and 15 m²mL⁻¹, 120 min, and 5 mL supernatant (see Fig. 3a). The SCI_i obtained for XAD16 (III, ($-\leftrightarrow\pm$)) and XAD7 (IV, ($\pm\leftrightarrow+$)) are compared regarding a significant difference representatively for categories ($-\leftrightarrow\pm$) and ($\pm\leftrightarrow+$) to decide on further screening experiments.

Table 2. Experimental results of adsorbent selection strategy.

Adsorbent	Surface area [m ² mL ⁻¹]	Experimental yield Y_{Caffeine} [%]	Peak area purity P [%]
HP20SS	15	91.88 ± 0.2	53.22 ± 0.01
HP20SS	5	68.35 ± 1.4	50.83 ± 0.4
HP20SS	1	15.60 ± 2.3	40.52 ± 0.3
SP207	15	98.01 ± 0.04	54.04 ± 0.06
SP207	5	80.77 ± 0.7	54.04 ± 0.1
SP207	1	20.50 ± 5.3	44.02 ± 1.5
XAD16	15	93.10 ± 0.08	53.58 ± 0.05
XAD16	5	66.38 ± 1.6	51.1 ± 0.1
XAD16	1	10.68 ± 7.8	48.39 ± 0.1
XAD7	15	65.46 ± 3.24	45.19 ± 0.1
XAD7	5	32.57 ± 1.34	34.26 ± 0.7
XAD7	1	8.59 ± 1.5	26.04 ± 0.7
Active carbon	15	99.94 ± 0.03	54.77 ± 0.1
Active carbon	5	97.01 ± 0.74	56.79 ± 0.12
Active carbon	1	24.00 ± 1.5	48.53 ± 0.41

Different SCI_i are due to varying performances regarding purity and yield (see Tab. 2). Because of decreasing purity compared to the initial purity of the system of about 55 %, the PPI_i for XAD7 (IV, ($\pm\leftrightarrow+$)) are negative for all surfaces tested and thus lie outside the scope of the SCI_i (see Fig. 4, Tab. 2). The minimal SCI_i value for XAD16 (III, ($-\leftrightarrow\pm$)) is about 39 €g_{Caffeine}⁻¹ for a surface of 15 m²mL⁻¹. Thus, groups II and IV are excluded from further screening. Following the methodology developed, HP20SS (I, ($-\leftrightarrow\pm$)) and SP207 (III, ($-\leftrightarrow\pm$)) are tested in the next screening run (see Fig. 3b). During the second screening, the SCI_i decreases for adsorption with SP207 (17.5 €g_{Caffeine}⁻¹) for 15 m²mL⁻¹ due to higher yields and slightly higher purities (see Fig. 4, Tab. 2). On the contrary, adsorption with HP20SS leads to a higher SCI_i (89.7 €g_{Caffeine}⁻¹) for 15 m²mL⁻¹ compared to XAD16 (III, ($-\leftrightarrow\pm$)) and SP207. Apparently, a steric effect is not inhibiting adsorption of the target component and selective adsorption is benefited by smaller pore sizes. Consequently, all adsorbents of group I are excluded from further screening (see Fig. 3c).

Due to the constant decrease of the SCI_i , active carbon (I/III, ($-\leftrightarrow\pm$)) is tested in the next screening run (see Fig. 3c). Since active carbon adsorbs the impurities and target component almost completely for a surface of 15 m²mL⁻¹, low purities and thus a PPI_i around 0.2 % results (see Tab. 2). Combining low PPI_i with yields of about 99 % ends up in SCI_i around 374 €g_{Caffeine}⁻¹. For active carbon the lowest SCI_i (71.5 €g_{Caffeine}⁻¹) is calculated for a surface of 5 m²mL⁻¹ (see Fig. 4). Since the minimal SCI_i of all adsorbents tested has been identified for the adsorption of caffeine with SP207, the search and screening terminates.

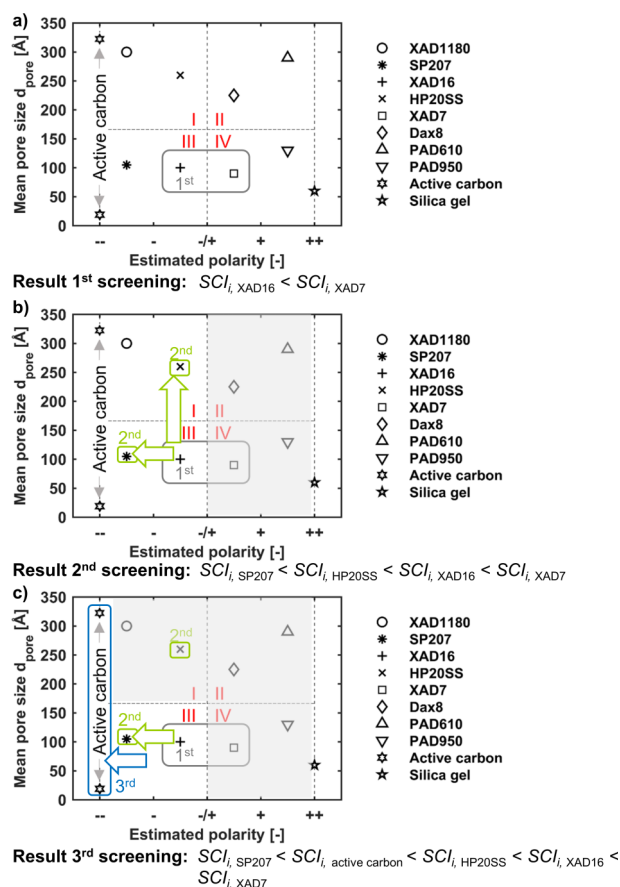


Figure 3. Screening order for adsorption of caffeine out of an aqueous solution. (a) First screening with XAD7 and XAD16 at varying surfaces of 1, 5, and 15 m²mL⁻¹ targeting at minimal SCI_i . The lower SCI_i is obtained for XAD16. (b) Stepwise screening of adsorbents with lower polarity and same pore size (III, ($-\leftrightarrow\pm$)), same polarity and higher pore size (I, ($-\leftrightarrow\pm$)). Fixing of mean pore size to small pores (III) based on the lowest SCI_i . Adjustment of search direction according to the SCI_i . (c) Screening of adsorbent with same pore size but different polarity. Search terminates due to increasing SCI_i of active carbon compared to SP207.

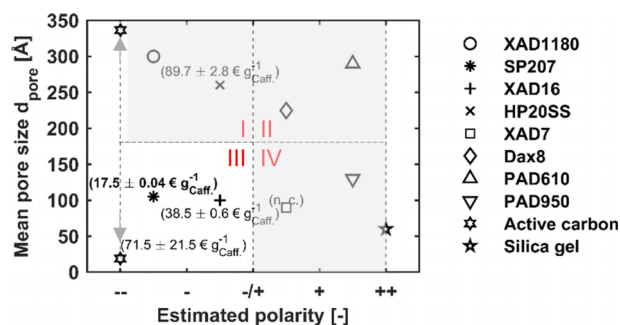


Figure 4. SCI_i for adsorption of caffeine out of an aqueous solution. The screening experiments are executed for varying specific surfaces (1, 5, and 15 m²mL⁻¹), 5 mL supernatant, 120 min adsorption time, and at room temperature (20–25 °C). For each adsorbent the lowest SCI_i of all surfaces screened is selected.

Overall caffeine is a medium polar component and thus it should adsorb preferably on the medium polar adsorbents in polarity sub-classes ($\leftrightarrow\pm$) and ($\pm\leftrightarrow$). Due to the structural similarity of the impurities and the target component, the low PPI_i values are not surprising, indicating a rather low selectivity of the adsorption step.

To verify the method developed, the full screening set of adsorbents is tested (Fig. 5). The highest yields in the polarity classes ($\pm\leftrightarrow$) around 80 % are generated for adsorption with Dax8 (II, ($\pm\leftrightarrow$)) and PAD610 (II, ($\pm\leftrightarrow$)) for a surface of $15\text{ m}^2\text{ mL}^{-1}$. The lowest SCI_i of group II and IV around $6007\text{ € g}_{\text{Caffeine}}^{-1}$ results for adsorption with PAD610 (see SI). Due to low yields and low or negative PPI_i , the SCI_i for high-polar adsorbents with low mean pore sizes (IV) are either not calculable or extremely high, indicating a high-cost adsorption step. The significantly higher SCI_i confirm and verify the early limitation of the adsorbents based on the results obtained from adsorption with XAD16 (III, ($\leftrightarrow\pm$)) and XAD7 (IV, ($\pm\leftrightarrow$)). Thus, these two adsorbents can be utilized for an initial guess concerning the adsorption behavior of high-polar ($\pm\leftrightarrow$) or low-polar ($\leftrightarrow\pm$) adsorbents.

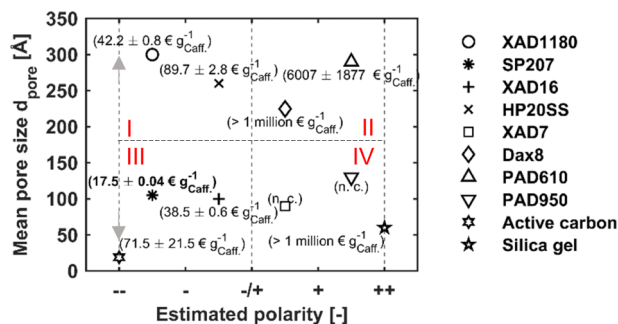


Figure 5. SCI_i for adsorption of caffeine out of an aqueous solution executed apart the robotic platform. The screening experiments are executed for varying specific surfaces (1, 5, and $15\text{ m}^2\text{ mL}^{-1}$), 5 mL supernatant, 120 min adsorption time, and at room temperature ($20\text{--}25\text{ °C}$). For each adsorbent the lowest SCI_i of all surfaces screened is selected.

4.2 Automation of Adsorbent Selection Strategy

After the verification of the general suitability of the methodology developed, the screening strategy is automated to further support and accelerate adsorption process design. The results of automatic experiments are shown in Fig. 6. Similar challenges to Schuldt and Schembecker [7] appeared during automated adsorption like static charge of the adsorbents during the solid dosing steps.

Comparing the SCI_i values of manual and automated experiments, differences can be identified resulting from slightly different yields and PPI_i (see Figs. 4 and 6 in SI). For example, the deviation of manual and automated experiments of HP20SS (I, ($\leftrightarrow\pm$)) and a specific surface of $1\text{ m}^2\text{ mL}^{-1}$ can be traced back to variation of the solid and liquid dosing steps of the manual experiments. The screening order is identical to the manual experiments (see Fig. 3) excluding group I, II, and IV. The automatic strategy is leading to SP207 (III, ($\leftrightarrow\pm$)) with the over-

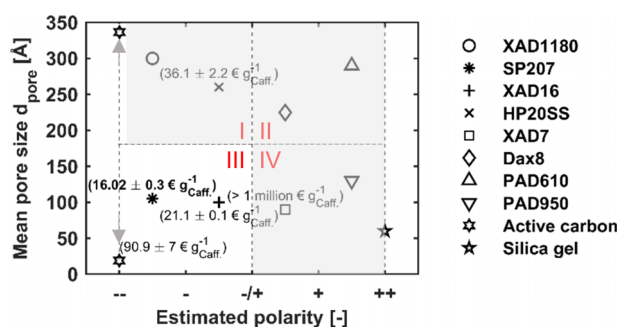


Figure 6. SCI_i for adsorption of caffeine out of an aqueous solution executed on the robotic platform. The screening experiments are executed for varying specific surfaces (1, 5, and $15\text{ m}^2\text{ mL}^{-1}$), 5 mL supernatant, 120 min adsorption time, and 25 °C . The SCI_i values shown are the corresponding lowest values for each adsorbent.

all lowest SCI_i of $16\text{ € g}_{\text{Caffeine}}^{-1}$ similar to the manual experiments. Hereby, the automation of the screening strategy is successfully validated.

The methodology is flexible and universally applicable to various purification purposes. The number of experiments is reduced by obtaining the degree of information necessary to select suitable adsorbents for liquid-phase adsorption. Automation further strengthens the methodology by minimizing manual effort and material consumption. Even more, the strategy can be executed autonomously either on the robotic platform or in a manual manner, since all decisions are well-founded and generalized by KPI. The results prove that the combination of KPI, the systematic strategy for adsorbent selection and automation, leads to efficient process design.

5 Conclusion and Outlook

This work outlines the necessity of a strategic and systematic methodology for adsorbent selection for liquid-phase adsorption. Complex mixtures, e.g., from biochemical reactions are demanding for simplified and systematic approaches to overcome the challenging broad and time-consuming screening of adsorbents.

Aiming at reduced number of experiments and minimized manual effort and time, a set of representative adsorbents was defined covering oxidic, polymeric, and carbon-based adsorbents. The set was categorized according to polarity and mean pore sizes in four groups of small/arge pore sizes and non-polar/polar adsorbents. Additionally, the surface area was varied for all adsorbents (1, 5, and $15\text{ m}^2\text{ mL}^{-1}$). A flexible and adapting screening strategy was developed directing to a minimal SCI_i . Automation on a robotic platform accelerated the screening procedure ending in autonomous decisions for suitable adsorbents founded by KPI.

For an aqueous model system with caffeine as target component, SP207 was identified as most promising adsorbent after a three-step screening procedure. For manual and automated experiments similar SCI_i values resulted around 16.2 and $17.5\text{ € g}_{\text{Caffeine}}^{-1}$ for a provided specific surface of $15\text{ m}^2\text{ mL}^{-1}$. Hereby, the methodology was successfully automated. To

increase the selectivity of the process leading to a higher PPI_i , the subsequent desorption step is crucial. For, e.g., a solvent-based desorption, the selection of wash and recovery solvent influences the overall efficiency of the process. Similar to approaches developed for extractant selection [6], desorbent screening could be executed systematically and automatically on a robotic platform as well.

A transfer to other systems seems to be reasonable, since the model system selected is already challenging due to the structural similarity of the components. For example, Winkelkemper et al. [18] performed an adsorbent screening for liquid-phase adsorption of bacatin III out of an aqueous supernatant with 13 contaminants. The screening set consisted of similar adsorbents indicating that the approach developed is applicable to different fermentation broths. The set can be extended by further adsorbents any time. Nevertheless, the qualitative matrix over pore size and polarity proved to be a reasonable simplification. Overall, the strategy accelerates adsorption design especially in early process design stages leading to overall efficient production processes.

Supporting Information

Supporting Information for this article can be found under DOI: <https://doi.org/10.1002/ceat.202200152>.

Acknowledgment

The research has received funding from the Federal Ministry of Education and Research (funding code: 161B0620). This work forms part of the Syntheroids project ("Synthetic biology for industrial production of steroids"; ERA-CoBioTech 1st call). The authors express their special thanks to Daniela Ermeling and Clemens Pietzsch for their support during the experiments. Open access funding enabled and organized by Projekt DEAL.

The authors have declared no conflict of interest.

Symbols used

PPI_i	[%]	purification performance index
SCI_i	[€ g ⁻¹]	separation cost indicator
x, P	[-]	purity
Y	[%]	yield

Greek letter

κ	[€ g ⁻¹]	cost factor
----------	----------------------	-------------

Sub- and superscripts

0	initial
conv.	conversion
f	final
i	step
in	inlet

nd	second
out	outlet
pore	pore
pur.	purification
rd	third
st	first

Abbreviations

HT	high throughput
KPI	key performance indicator
SPE	solid-phase extraction

References

- [1] T. C. Silva, M. Eppink, M. Ottens, *J. Chem. Technol. Biotechnol.*, in press. DOI: <https://doi.org/10.1002/jctb.6792>
- [2] J. A. Selekmán, J. Qiu, K. Tran, J. Stevens, V. Rosso, E. Simmons, Y. Xiao, J. Janey, *Annu. Rev. Chem. Biomol. Eng.* **2017**, *8*, 525–547. DOI: <https://doi.org/10.1146/annurev-chem-bioeng-060816-101411>
- [3] C. Stamatis, S. Goldrick, D. Gruber, R. Turner, N. J. Titchener-Hooker, S. S. Farid, *J. Chromatogr. A* **2019**, *1596*, 104–116. DOI: <https://doi.org/10.1016/j.chroma.2019.03.005>
- [4] S. K.-F. Wong, Y. Lu, W. Heineman, J. Palmer, C. Courtney, *J. Biomol. Screening* **2005**, *10* (5), 524–531. DOI: <https://doi.org/10.1177/1087057105275457>
- [5] M. Alexovič, Y. Dotsikas, P. Bober, J. Sabo, *J. Chromatogr. B* **2018**, *1092*, 402–421. DOI: <https://doi.org/10.1016/j.jchromb.2018.06.037>
- [6] M. Schreiber, M. Brunert, G. Schembecker, *Chem. Eng. Technol.* **2021**, *44* (9), 1578–1584. DOI: <https://doi.org/10.1002/ceat.202100171>
- [7] S. Schuldt, G. Schembecker, *Chem. Eng. Technol.* **2013**, *36* (7), 1157–1164. DOI: <https://doi.org/10.1002/ceat.201200725>
- [8] T. Wu, Y. Zhou, *J. Lab. Autom.* **2014**, *19* (4), 381–393. DOI: <https://doi.org/10.1177/2211068213499756>
- [9] F. Biermann, J. Mathews, B. Niefing, N. König, R. H. Schmitt, *Processes* **2021**, *9* (6), 966. DOI: <https://doi.org/10.3390/pr9060966>
- [10] H. Morschett, N. Tenhaef, J. Hemmerich, L. Herbst, M. Spiertz, D. Dogan, W. Wiechert, S. Noack, M. Oldiges, *Biotechnol. Bioeng.* **2021**, *118* (7), 2759–2769. DOI: <https://doi.org/10.1002/bit.27795>
- [11] R. Bogue, *Ind. Robot* **2012**, *39* (2), 113–119. DOI: <https://doi.org/10.1108/01439911211203382>
- [12] J. L. Coffman, J. F. Kramarczyk, B. D. Kelley, *Biotechnol. Bioeng.* **2008**, *100* (4), 605–618. DOI: <https://doi.org/10.1002/bit.21904>
- [13] Y. Yan, L. Ai, H. Zhang, W. Kang, Y. Zhang, K. Lian, *Microchem. J.* **2021**, *165*, 106142. DOI: <https://doi.org/10.1016/j.microc.2021.106142>
- [14] S. Dugheri, G. Marrubini, N. Mucci, G. Cappelli, A. Bonari, I. Pompilio, L. Trevisani, G. Arcangeli, *Acta Chromatogr.* **2021**, *33* (2), 99–111. DOI: <https://doi.org/10.1556/1326.2020.00790>
- [15] R. Bhambure, K. Kumar, A. S. Rathore, *Trends Biotechnol.* **2011**, *29* (3), 127–135. DOI: <https://doi.org/10.1016/j.tibtech.2010.12.001>

- [16] M. B. Ahmed, J. L. Zhou, H. H. Ngo, W. Guo, *Sci. Total Environ.* **2015**, 532, 112–126. DOI: <https://doi.org/10.1016/j.scitotenv.2015.05.130>
- [17] L. Estupiñan Perez, A. M. Avila, J. A. Sawada, A. Rajendran, S. M. Kuznicki, *Sep. Purif. Technol.* **2016**, 168, 19–31. DOI: <https://doi.org/10.1016/j.seppur.2016.05.010>
- [18] T. Winkelkemper, S. Schultdt, G. Schembecker, *Sep. Purif. Technol.* **2011**, 77 (3), 355–366. DOI: <https://doi.org/10.1016/j.seppur.2011.01.004>
- [19] S. Sadighi, M. S. Alivand, M. Faghihi, *Pet. Coal* **2019**, 61 (5), 932–948.
- [20] F. B. Thygs, J. Merz, G. Schembecker, *Chem. Eng. Technol.* **2016**, 39 (6), 1049–1057. DOI: <https://doi.org/10.1002/ceat.201500572>
- [21] T. Winkelkemper, G. Schembecker, *Sep. Purif. Technol.* **2010**, 72 (1), 34–39. DOI: <https://doi.org/10.1016/j.seppur.2009.12.025>
- [22] N. Abdehagh, F. H. Tezel, J. Thibault, *Adsorption* **2016**, 22 (3), 357–370. DOI: <https://doi.org/10.1007/s10450-016-9784-y>
- [23] I. Lukin, G. Jach, I. Wingartz, P. Welters, G. Schembecker, *J. Agric. Food Chem.* **2019**, 67 (49), 13412–13419. DOI: <https://doi.org/10.1021/acs.jafc.8b07270>
- [24] *Microbial Steroids: Methods and Protocols* (Eds: J.-L. Barredo, I. Herráiz), Methods in Molecular Biology, Vol. 1645, Springer, New York **2017**.
- [25] *Adsorptionstechnik* (Eds: D. Bathen, M. Breitbach), VDI-Buch, Springer, Berlin **2001**.
- [26] W. J. Thomas, *Adsorption Technology and Design*, 1st ed., Elsevier Science & Technology, Oxford **1998**.